Arab J Sci Eng (2015) 40:3263–3272
DOI 10.1007/s13369-015-1661-6

RESEARCH ARTICLE - MECHANICAL ENGINEERING

A Modified Particle Swarm Optimization Technique for Crack Detection in Cantilever Beams

Prabir K. Jena[1] · **Dayal R. Parhi**[1]

Received: 19 October 2014 / Accepted: 13 April 2015 / Published online: 28 April 2015

Abstract An inverse analysis of the crack identification problem is investigated by the modified particle swarm optimization (MPSO) technique. The objective of the present analysis is to predict the unknown crack location and its depth from the knowledge of frequency data obtained from theoretical and experimental investigation. In this paper, the proposed modified PSO (MPSO) mechanism employs the strategy of squeezing the physical domain of the search space in each iteration to accelerate the search process while maintaining the inherent structure of PSO algorithm. Analytical and experimental results of the cracked beam structure are compared with those obtained by modified PSO (MPSO) to ensure the integrity of the algorithm. To show its effectiveness, the results of the MPSO are compared with the results obtained by differential evolution. Simulation results reveal the better performance of the proposed algorithm in terms of predicting the location and depth of the crack.

Keywords Beam · Crack detection · Natural frequencies · Particle swarm optimization · Differential evolution

1 Introduction

The vibration-based structural damage detection problem using non-destructive inspection techniques have been the main thrust in the area of research for a long period. In order to obtain accurate predictions of crack through such techniques, a prior knowledge of the damage vicinity is required. The above limitations have made the vibration-based inspection methods very popular and important in crack detection. The existence of damage in the form of a small crack in a structure affects its dynamic characteristics such as natural frequencies and mode shapes. Therefore the natural frequencies and mode shapes of the structure could be used as a source of information regarding damage location and the extent of damage.

There are two approaches of thoughts in structural damage identification: the forward-based approach and the inverse approach. Normally, a forward-based approach involves the formulation of a mathematical model for the structure to demonstrate the structural behaviour and establish interrelations between the damage parameter and changes in structural dynamic characteristics such as natural frequencies and mode shapes. Kim and Stubbs [1] studied the effect of crack parameters on natural frequencies to decide the crack occurrence in thin cracked beams. Dimarogonas and Papadopoulos [2] derived a local stiffness matrix at the crack location to investigate the change in dynamic properties such as natural frequencies and mode shapes. Qian et al. [3] formulated the stiffness matrix of the beam containing an open-edge crack by integrating over stress intensity factors. Derived from the work of Qian et al. [3], Nahvi and Jabbari [4] identified the crack location and estimated the damage severity in a cantilever beam. Chondros et al. [5] developed a continuous cracked beam vibration theory to analyse lateral transverse vibration of the cracked Euler–Bernoulli beam with single-edge or double-edge open cracks. Orhan [6] studied the free and forced vibration analysis of a single- and two-edge cracked cantilever beam to describe the interdependency of natural frequencies to crack location and crack depth. Saavedra and Cuitino [7] used strain energy density function as an approach to deducing a finite element stiff-

✉ Prabir K. Jena
prabirkumarjena07@gmail.com

Dayal R. Parhi
dayalparhi@yahoo.com

[1] Department of Mechanical Engineering, National Institute of Technology, Rourkela, 769008 Odisha, India

ness matrix to study the dynamic response of different beams containing a transverse crack. Based on their work Zheng et al. [8] obtained natural frequencies and mode shapes of a cracked beam using finite element method by considering the stiffness matrix of an intact beam. Rizos et al. [9] modelled the crack using a rotational spring to predict the damage site and its severity in a cantilever beam. Extending the work of Rizos et al. [9], Gomes and Almeida [10] developed an analytical dynamic model for cracked beam to predict natural frequencies variations for several damage scenarios along the beam with various end conditions. Behzad et al. [11] presented a vibration-based algorithm for detection of multiple edge cracks in a cantilever beam. In this work, the crack was modelled as massless rotational spring in order to demonstrate a relationship between natural frequencies, crack locations and stiffness of equivalent springs. Nguyen [12] used mode shapes of a cracked beam to determine the depth and position of the crack. In this study, the finite element method was applied to analyse the mode shapes of a cracked beam using the 3D beam element that helps to inspect a small crack by using the projections of the mode shapes on appropriate planes.

In the last decades, inverse approach algorithms have gained popularity and proved to be efficient in solving crack detection problems using vibration signatures that are discussed in the following literatures. Sahoo and Maity [13] proposed a hybrid neuro-genetic algorithm to determine crack parameters in beam and frame structures by investigating the variations in natural frequencies and strains. Dash and Parhi [14] designed a smart hybrid system for detecting cracks in a cantilever beam. In this work, the calculated natural frequencies and mode shapes are used to design and train the hybrid genetic algorithm and fuzzy logic controller in order to predict the crack location and the crack depth. Aydin and Kisi [15] presented a fault diagnosis method which uses beam properties, beam end conditions and vibration parameters as inputs to a neural network (NN) to predict the location and severity of cracks. Vakil-Baghmisheh et al. [16] implemented a genetic algorithm to estimate crack location and depth in beam-like structures. Rong and Shun [17] successfully implemented an adaptive real-parameter genetic algorithm combined with simulated annealing to identify cracks in beam-like structures for different boundary conditions and damage situations. Khaji and Mehrjoo [18] implemented a genetic algorithm as an inverse approach to estimating depth and location of cracks in beam-like structures from the knowledge of natural frequencies and modeshapes. More recently, there is a growing preference for another population-based evolutionary optimization technique known as differential evolution (DE) [19] over genetic algorithm (GA) in solving crack detection problems. Casciati [20] applied differential evolution algorithms to detect damage occurrence by comparing stiffness matrices of damaged and undamaged cantilever beams. The drawbacks of above-discussed algorithms are slow and premature convergence towards globally optimal solution. The particle swarm optimization (PSO), first proposed by Kennedy and Eberhart [21], is a novel population-based global optimization technique motivated by an intelligent social system. Recently PSO has been successfully implemented to many damage detection problems [22–28].

In this paper, an alternative technique is proposed to the crack detection problem using a modified PSO (MPSO). The proposed MPSO employs a time-dependent search space squeezing strategy to deal with inequality constraints and to improve the convergence speed. The proposed MPSO has two advantages over the dynamic search space reduction strategy [29]. The first one is that the margins by which the reduction in the search space from both the sides of problem variables (i.e., crack location and crack depth) takes place, depend upon the iteration number, unlike the predetermined step size considered in the dynamic search space reduction strategy [29]. The second advantage is that the boundary of the search space is determined from the relative distance measured from the global best position. To examine the potential of the proposed MPSO, the crack identification problem was investigated and the results obtained compared with those obtained by using DE.

In this paper, the Cracked beam system modelling is presented in the following section, while an inverse approach for the crack identification problem is described in Sect. 3. The analysis of modified time-dependent computational search space squeezing strategy is presented in Sect. 4. The experimental setup and the results thereby obtained are set forth in Sect. 5. The results obtained by means of numerical simulations are discussed in Sect. 6. The paper is concluded in Sect. 7.

2 Cracked Beam System Modelling

A cantilever beam of length L, height T, width W, and a transverse open-edge full-width crack of depth b_1, at a variable position L_c is shown in Fig. 1. The presence of a transverse surface crack introduces local flexibility which influences its dynamic performance of the structure. The coefficients of the flexibility matrix are expressed by the stress intensity factors. The relationship between the strain energy release rate J and stress intensity factors, $G_{\mathrm{I}i}$, at the crack section is expressed by Eq. (1).

$$J = \frac{1}{E}\left(G_{\mathrm{I}1} + G_{\mathrm{I}2}\right)^2 \tag{1}$$

where $G_{\mathrm{I}1}$ and $G_{\mathrm{I}2}$ are stress intensity factors for opening mode I due to loads P_1 and P_2, respectively. These factors are expressed by [30]:

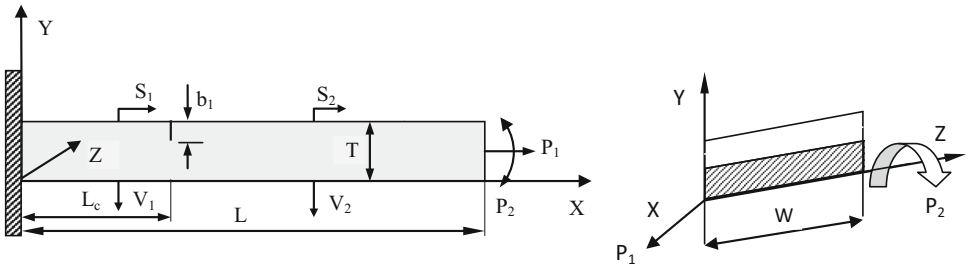

Fig. 1 Cantilever beam with a crack at L_c. L is the length of the beam; b_1 is the crack depth; T is the beam height; S_1 and S_2 are the longitudinal vibrations; V_1 and V_2 represents the transverse vibrations

$$G_{I1} = \frac{P_1}{WT}\sqrt{\pi b}\left(F_1\frac{b}{T}\right);$$

$$G_{I2} = \frac{6P_2}{WT^2}\sqrt{\pi b}\left(F_2\left(\frac{b}{T}\right)\right); \quad 0 < b < b_1$$

$$F_1\left(\frac{b}{T}\right) = \left(\frac{2T}{\pi b}\tan\left(\frac{\pi b}{2T}\right)\right)^{0.5} \times\left\{\frac{0.752+2.02\,(b/T)+0.37\,(1-\sin\,(\pi b/2T))^3}{\cos\,(\pi b/2T)}\right\}$$

$$F_2\left(\frac{b}{T}\right) = \left(\frac{2T}{\pi b}\tan\left(\frac{\pi b}{2T}\right)\right)^{0.5} \times\left\{\frac{0.923+0.199\,(1-\sin\,(\pi b/2T))^4}{\cos\,(\pi b/2T)}\right\}$$

The local stiffness matrix can be obtained by taking the inverse of the flexibility matrix as given by Dimarogonas and Papadopoulos [2].

$$K = \begin{bmatrix} K_{11} & K_{12} \\ K_{21} & K_{22} \end{bmatrix} = \begin{bmatrix} C_{11} & C_{12} \\ C_{21} & C_{22} \end{bmatrix}^{-1}$$

2.1 System Equations for Bending Vibration

The free vibration of an Euler–Bernoulli beam with a constant rectangular cross section is given by the following differential equations as:

$$EI\frac{\partial^4 V}{\partial x^4} + \rho A\frac{\partial^2 V}{\partial t^2} = 0 \tag{2}$$

$$\left(\frac{E}{\rho}\right)\frac{\partial^2 S}{\partial x^2} = \frac{\partial^2 S}{\partial t^2} \tag{3}$$

Equation (2) represents for transverse vibration, and Eq. (3) represents for longitudinal vibration. Where S and V represent the longitudinal and transverse displacements; ρ is the density; and A is the cross-sectional area of the beam. Equations (2) and (3) hold good for the two segments of the cracked beam.

The normal functions for the cracked beam model (Fig. 1) in non-dimensional form for both longitudinal and bending vibration in steady state can be expressed by:

$$\overline{V}_1(\overline{x}) = B_1\cosh\left(\overline{H}_v\overline{x}\right) + B_2\sinh\left(\overline{H}_v\overline{x}\right) + B_3\cos(\overline{H}_v\overline{x}) + B_4\sin\left(\overline{H}_v\overline{x}\right) \tag{4a}$$

$$\overline{V}_2(\overline{x}) = B_5\cosh\left(\overline{H}_v\overline{x}\right) + B_6\sinh\left(\overline{H}_v\overline{x}\right) + B_7\cos\left(\overline{H}_v\overline{x}\right) + B_8\sin\left(\overline{H}_v\overline{x}\right) \tag{4b}$$

$$\overline{S}_1(\overline{x}) = B_9\cos\left(\overline{H}_s\overline{x}\right) + B_{10}\sin\left(\overline{H}_s\overline{x}\right) \tag{4c}$$

$$\overline{S}_2(\overline{x}) = B_{11}\cos\left(\overline{H}_s\overline{x}\right) + B_{12}\sin\left(\overline{H}_s\overline{x}\right) \tag{4d}$$

where

$$\overline{x} = \frac{x}{L};\quad \overline{S} = \frac{S}{L};\quad \overline{V} = \frac{V}{L};\quad \alpha = \frac{L_c}{L}$$

$$\overline{H}_s = \left(\frac{\omega L}{D_s}\right)^{1/2};\quad D_s = \left(\frac{E}{\rho}\right)^{1/2};$$

$$\overline{H}_v = \left(\frac{\omega L^2}{D_v}\right)^{1/2};\quad D_v = \left(\frac{EI}{\mu}\right)^{1/2};\quad \mu = A\rho$$

The B_i, $(i = 1, 12)$ are constant coefficients that can be determined from the boundary conditions.

Geometric natural boundary conditions at both ends are:

$$\overline{S_1}(0) = 0;\quad \overline{V_1}(0) = 0;\quad \overline{V}_1'(0) = 0 \tag{5a}$$

$$\overline{S}_2'(1) = 0;\quad \overline{V}_2''(1) = 0;\quad \overline{V}_2'''(1) = 0 \tag{5b}$$

Compatibility conditions are introduced to impose continuity of displacement, bending moment and shear forces of the two segments at the crack location, $x = L_c$. These conditions are given by:

$$\overline{S}_1(\alpha) = \overline{S}_2(\alpha);\quad \overline{V}_1(\alpha) = \overline{V}_2(\alpha);\quad \overline{V_1}''(\alpha) = \overline{V_2}''(\alpha);\quad \overline{V_1}'''(\alpha) = \overline{V_2}'''(\alpha) \tag{5c}$$

The existence of the difference in the slopes at the crack location imposes additional equilibrium conditions of force balance and moment balance are given by the following relations in terms of local stiffness matrix, K of the cracked beam.

$$AE\overline{S}_1'(\alpha) = K_{11}\left(\overline{S}_2(\alpha) - \overline{S}_1(\alpha)\right) + K_{12}\left(\overline{V_2}'(\alpha) - \overline{V_1}'(\alpha)\right)$$

$$\Rightarrow N_1N_2\overline{S}_1'(\alpha) = N_2\left(\overline{S}_2'(\alpha) - \overline{S}_1'(\alpha)\right)$$

$$+ N_1\left(\overline{V}'_2(\alpha) - \overline{V}'_1(\alpha)\right) \tag{5d}$$

$$EI\overline{V}''_1(\alpha) = K_{21}\left(\overline{S}_2(\alpha) - \overline{S}_1(\alpha)\right) + K_{22}\left(\overline{V}'_2(\alpha) - \overline{V}'_1(\alpha)\right)$$

$$\Rightarrow N_3N_4\overline{V}''_1(\alpha) = N_3\left(\overline{S}_2(\alpha) - \overline{S}_1(\alpha)\right) + N_4\left(\overline{V}'_2(\alpha) - \overline{V}'_1(\alpha)\right) \tag{5e}$$

where

$$N_1 = \frac{AE}{LK_{11}};\quad N_2 = \frac{AE}{K_{12}};\quad N_3 = \frac{EI}{LK_{22}} \text{ and } N_4 = \frac{EI}{L^2K_{21}}$$

The normal functions, Eq. (1), and the boundary conditions as mentioned above, yield the characteristic equation of the system as $|\Omega| = 0$, where Ω is a 12×12 matrix whose determinant is a function of natural circular frequency, ω; the non-dimensional location of the crack, α; and the local stiffness matrix, K, which in turn is a function of the non-dimensional crack depth, $\beta = \frac{b_1}{T}$. The above theoretical study was used to determine the changes in natural frequencies of a beam due to a crack placed at a specific location and possessing a known depth.

3 An Inverse Approach for Crack Identification

As discussed in the previous sections, determination of the changes in the natural frequencies of beams from a given value of crack location and crack depth is a straightforward task. The objective of the inverse approach is to estimate the unknown crack location and its depth iteratively, using an optimization algorithm that results in a negligible difference between the actual and the estimated natural frequencies. The solution of the present inverse problem is achieved by minimizing the objective function expressed by:

$$\min\ f(l,d) = \sum_{i=1}^{n}\left|\varphi_i\left(f_i^d - f_i^e\right)\right| \tag{6}$$

Subject to the constraints $0 < b_1 < T$ and $0 < L_c < L$.

In this equation, φ_i is the ith weighting factor; f_i^d is the ith desired natural frequency of the cracked beam; f_i^e refers to the ith natural frequency estimated from the algorithm and n is the number of natural frequencies used to evaluate the objective function. In the present work, the first three natural frequencies of the beam are used as inputs to the crack detection problem to evaluate the objective function. The value of weighting factor is assumed to be $1/i$ [20] in order to assign greater degree of importance to the lower modes. In the present study, a modified PSO (MPSO) has been developed and used for crack identification. In the following section, a brief description about PSO and the proposed MPSO is presented.

3.1 Methodologies

3.1.1 Particle Swarm Optimization

Particle swarm optimization (PSO) proposed by Kennedy and Eberhart [21] is an evolutionary optimization technique, motivated by the social interaction of animals such as bird flocking, fish schooling and swarm theory. PSO utilizes a population-based global search procedure, in which each individual is treated as particles of the population to share information among them, which improves the efficiency of the search process to reach at the global optimum.

In the PSO with N particles, each particle explores a possible solution in a D-dimensional problem search space with the position vector and velocity vector of particle i at the kth iteration represented as $X_i(k) = [x_{i1}(k), x_{i2}(k), \ldots, x_{iD}(k)]$ and $V_i(k) = [v_{i1}(k), v_{i2}(k), \ldots, v_{iD}(k)]$. Each dimension in D-dimensional search space corresponds to a problem variable in a function being optimized. The updated velocity and position of particle i at $(k+1)$th iteration are modified under the following equation in the PSO algorithm:

$$v_{ij}(k+1) = w \times v_{ij}(k) + c_1 \times rand_1 \times [pbest_{ij}(k) - x_{ij}(k)] + c_2 \times rand_2 \times [gbest_j(k) - x_{ij}(k)] \tag{7}$$

$$x_{ij}(k+1) = x_{ij}(k) + v_{ij}(k+1) \tag{8}$$

for $i = 1, 2, \ldots, N$; $j = 1, 2, \ldots, D$, where c_1 (cognitive parameter) and c_2 (social parameter) are known as acceleration coefficients, that tunes the relative proportion of cognitive and social interactions to drag particle towards *pbest* and *gbest* position. In this paper, the acceleration coefficients are updated using the following relations:

$$c_1 = c_{1i} - (c_{1i} - c_{1f}) \times \left(\frac{k}{MAX\_ITER}\right) \tag{9}$$

$$c_2 = c_{2i} + (c_{2f} - c_{2i}) \times \left(\frac{k}{MAX\_ITER}\right) \tag{10}$$

where c_{1i}; c_{1f}; c_{2i}; and c_{2f} are initial and final values of cognitive and social components of acceleration factors, respectively. In the above equation, k is the current iteration and *MAX_ITER* is the maximum number of allowable iterations.

In the present work, the inertia weight parameter w is expressed as a function of the iteration number. The initial value of w is set to $w_{\max}$ and reduced linearly to $w_{\min}$ according to:

$$w = w_{\max} - (w_{\max} - w_{\min}) \times \left(\frac{k}{MAX\_ITER}\right) \tag{11}$$

Vector $pbest_i(k) = [pbest_{i1}(k), pbest_{i2}(k), \ldots, pbest_{iD}(k)]$ is the best previous position achieved by the ith particle, which is called as personal best (*pbest*) position, while the position of the best particle explored by the entire population is represented as the global best (*gbest*) position, which is denoted by the vector $gbest(k) = [gbest_1(k), gbest_2(k), \ldots, gbest_D(k)]$

The parameters $rand_1$ and $rand_2$ are two distinct random numbers in the range [0,1].

For the present minimization optimization problem,

$$pbest_i(k) = \begin{cases} x_i(k) & \text{if } f[x_i(k)] < f[pbest_i(k-1)] \\ pbest_i(k-1) & \text{if } f[x_i(k)] > f[pbest_i(k-1)] \end{cases}$$

4 Analysis of Modified Time-Dependent Computational Search Space Squeezing Strategy

In the conventional PSO, the particle always covers the whole search area, thus increasing the computing time needed to reach a global optimum. Therefore, intelligent selection of the search space is desirable in order to improve convergence speed and to ensure a better performance of the algorithm by avoiding the solution being trapped in local optima. In the present investigation, the search space is readjusted based on the relative distance between *gbest*, lower and upper limits of the problem variables (i.e, crack location and crack depth). The limits of crack location and crack depth at the $(k+1)$th iteration are determined as follows:

$$x_{j,\max}(k+1) = x_{j,\max} - (x_{j,\max} - gbest_j(k)) \times \frac{k}{MAX\_ITER} \quad (12)$$

$$x_{j,\min}(k+1) = x_{j,\min} + (gbest_j(k) - x_{j,\min}) \times \frac{k}{MAX\_ITER} \quad (13)$$

$x_{j,\max}$ and $x_{j,\min}$ are the maximum and minimum limits of the problem variables in the computational domain of the search space. The application of MPSO algorithm to the crack detection problem is described in the following section. The crack detection procedure starts with N number of particles with the position vector x_j of each particle which is described by the randomly generated unknown pairs of crack location and crack depth. By utilizing the concept of squeezing of computational search domain, the optimal pairs of crack location and crack depth could be obtained by evaluating the objective function, i.e., Eq. (6) until the stopping criterion is met.

The convergence criterion is defined as the computational error of 10^{-3} or a predefined number of iterations is reached.

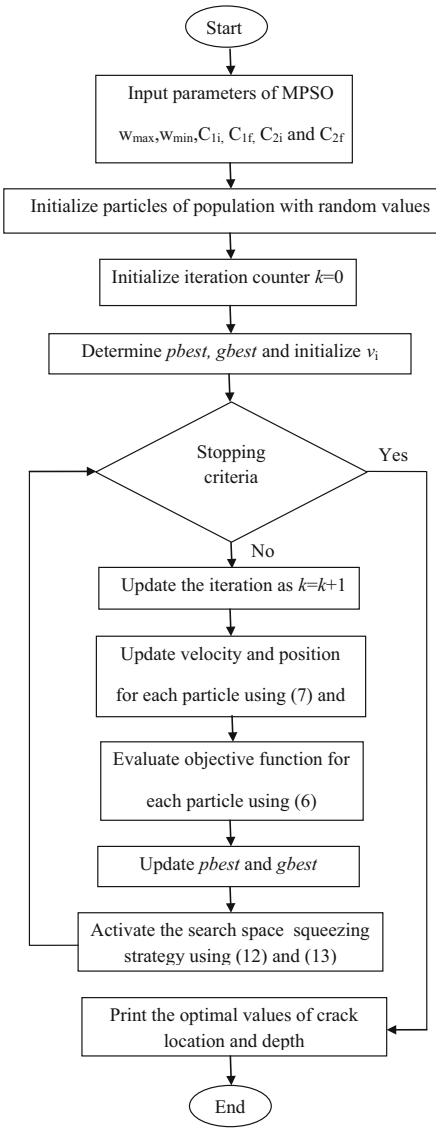

Fig. 2 Flow chart of the proposed MPSO algorithm

4.1 Implementation of MPSO for Crack Identification Problem

The flow chart of proposed MPSO is illustrated in Fig. 2. The steps followed for solving crack identification problem using MPSO algorithm are as follows.

Step 1 Crack location and crack depth, the decision variables in the crack identification problem are represented with the position of particles by satisfying the constraints of each variables. Initial position of particle i is created randomly as follows

$$x_{ij} = x_{j,\min} + r \times \left(x_{j,\max} - x_{j,\min}\right) \quad (14)$$

where r is a random number between 0 and 1.

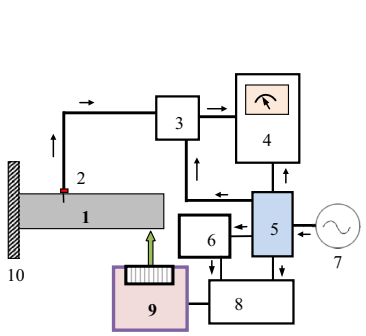

Fig. 3 Schematic block diagram of experimental setup for cantilever beam

Step 2 Evaluate the objective function (fitness function) of individual particle from Eq. (6) to obtain the optimal pairs of crack location and crack depth by minimizing it.
Step 3 Evaluation of fitness values using Eq. (6) for the initial particles of the swarm are set as the initial *pbest* values of the particles. The best evaluation value among all the *pbest* values is denoted as *gbest*.
Step 4 Update velocity by Eq. (7) and position by Eq. (8).
Step 5 Evaluate the fitness value of each particle according to its updated position. Evaluation value of each particle is compared with the previous *pbest* in order to update *pbest*. Then find *gbest* position among particles.
Step 6 Activate the squeezing strategy to regulate the upper and lower boundaries of the particles in each iteration relative to *gbest* position using Eqs. (12) and (13).
Step 7 The algorithm will be terminated if the stopping criterion is reached, otherwise it is continued from *Step 4*.

5 Experimental Studies

To verify the integrity of the proposed crack detection method and to figure out the unavoidable errors associated with modelling and measurements, several experiments have been conducted in the laboratory. Figure 3 shows a schematic diagram of the experimental setup and its description. A cracked cantilever beam has been rigidly clamped to a concrete foundation base. The free end of the beam is excited with a vibration exciter. The vibration exciter is excited by the signal from the function generator. The signal is amplified by a power amplifier before being fed to the vibration exciter. The amplitudes of vibration of the non-cracked and the cracked cantilever beams are taken by using an accelerometer and are fed to the vibration indicator for analysis.

Several tests were conducted using the experimental setup on aluminium beam specimens (800 × 50 × 6) mm with a transverse crack to determine the natural frequencies for different crack locations (i.e., 50 mm, at 300 mm from the clamped end) and crack depths varying from 1.2 to 2.4 mm by a step of 0.6 mm. The cracks were prepared by fine saw cuts perpendicular to the longitudinal axis. This ensures that the crack remains open during the vibrations. These specimens are set to vibrate under the first, the second and the third modes of vibration. Experimental results for frequencies of transverse vibration at various locations along the length of the beam are recorded by positioning the vibration pick-up and tuning the vibration generator at the corresponding resonant frequencies. At each step, the first three bending natural frequencies of the cracked beams were measured. Table 1 gives the corresponding bending natural frequencies of the cracked beams.

Table 1 Measured natural frequencies for six experimental cases

Crack		Natural bending frequencies (Hz)		
Loc. (mm)	Dep. (mm)	f_1	f_2	f_3
50	1.2	7.281	45.906	127.523
50	1.8	7.234	45.465	127.263
50	2.4	7.157	45.123	127.041
300	1.2	7.304	45.765	127.857
300	1.8	7.288	45.577	127.177
300	2.4	7.255	45.239	126.627

The accuracy of the suggested method to determine the severity and the location of the damage was verified by comparing the natural frequencies of the damaged beam determined experimentally with the ones obtained through the cracked beam model developed to evaluate the objective function as discussed in Sect. 3.

6 Results and Discussion

6.1 Influence of the Crack on Vibration Characteristics

In this section, a method for solving the crack identification problem by the modified particle swarm optimization (MPSO) algorithm is discussed. The aim of this formulation is to determine the crack location and the crack depth by evaluating the objective function based on the natural frequencies of the beam, which makes it necessary to carry out the theoretical study prior to the optimization process in order to estimate the natural frequencies of the beam for different crack conditions.

In the present study, an aluminium beam was used to determine the changes in natural frequencies for different crack locations by means of an analytical method. The geometry and mechanical properties of the beam were the same for both the analytical and the experimental study. These properties

Table 2 Material properties and geometry of aluminium-alloy-2014-T_4 beam

Young's modulus, E	Density, ρ	Poisson's ratio, μ	Length, L	Width, W	Beam height, T
72.4 GPa	2.8 gm/cc	0.33	800 mm	50 mm	6 mm

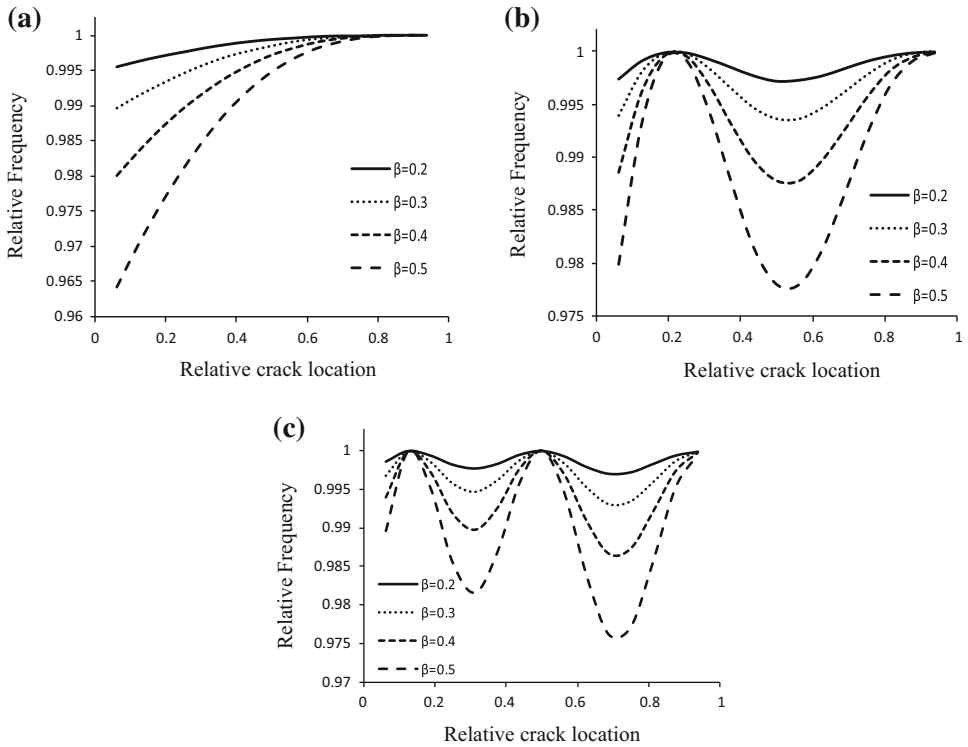

Fig. 4 Variation of relative frequencies with location and depth. **a** First mode of vibration, **b** second mode of vibration, **c** third mode of vibration

are set forth in Table 2. The first three relative natural frequencies of a cracked beam at the relative crack location $\alpha(L_c/L)$, for a crack of constant depth $\beta(b_1/T = 0.2, 0.3, 0.4$ and $0.5)$ are presented in Fig. 4. In this figure, it can be seen that the relative frequency for the first mode of vibration increases with respect to the relative position of the crack and decreases with respect to the relative crack depth. While, for the two other modes of vibration, minimum and maximum relative frequencies occur at distinct crack locations. It is also apparent from this figure, as well as from Fig. 5, that the deeper the crack, the larger the drop in the relative natural frequency.

The changes in mode shapes due to the presence of a crack at a specific location are presented in Fig. 6. As it can be seen in this figure, these changes increase with the severity of the crack.

The natural frequencies obtained from the solution of theoretical study were used as input for the inverse analysis, which is implemented by using MPSO. The computational efficiency of this method is verified by comparing its results with the ones obtained by using DE.

The control parameters selected for performance evaluation of different strategies are described as follows:

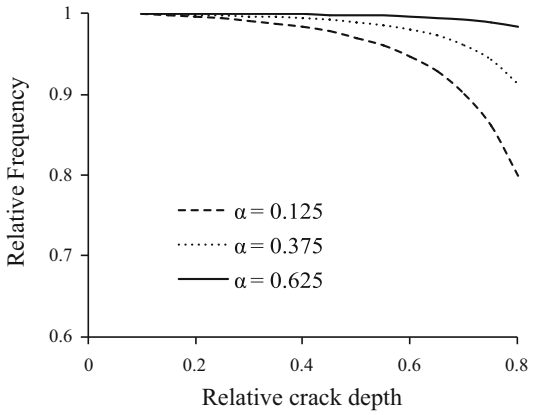

Fig. 5 First mode frequency variation with relative crack depth

For the MPSO, $w_{\max} = 0.9$; $w_{\min} = 0.4$; $c_{1i} = 2.0$; $c_{1f} = 0.5$; $c_{2i} = 0.5\, c_{2f} = 2.0$, size of population, $N = 10$; $MAX\_ITER = 100$. Similarly, the control parameters for DE are the scaling factor $F = 0.5$ and the crossover constant $CR = 0.8$.

Two crack sizes at three different locations in the beam are used in order to compare the performance of the proposed

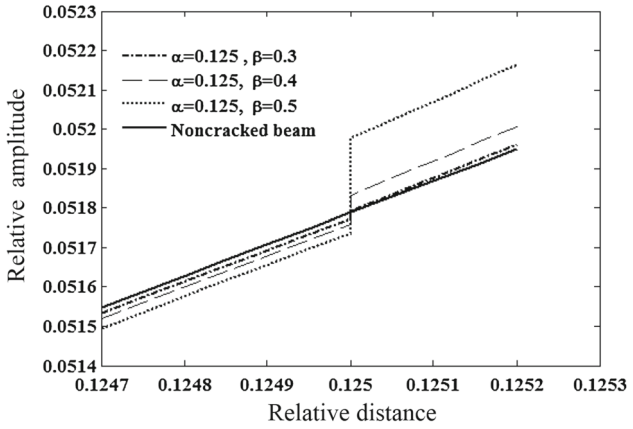

Fig. 6 Magnified view of jump in mode shape at the relative crack location for first mode of vibration

Table 3 Theoretical crack cases and corresponding natural frequencies

Case no.	Crack (mm)		Natural bending frequencies (Hz)		
	Location	Depth	f_1	f_2	f_3
1	No crack	No depth	7.6829	48.1669	134.8128
2	200	1.8	7.6413	48.1360	134.248
3	400	1.8	7.6717	47.8427	134.812
4	600	1.8	7.6819	48.0418	133.933
5	200	2.4	7.6026	48.1259	133.726
6	400	2.4	7.6612	47.5604	134.812
7	600	2.4	7.6809	47.9422	133.115

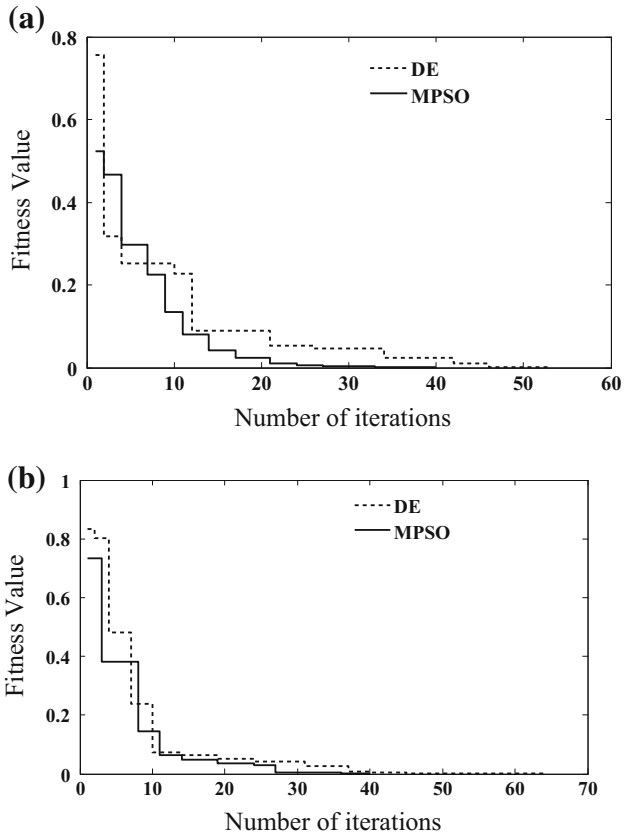

Fig. 7 **a** and **b** Convergence characteristics of MPSO and DE algorithm for crack case no. 2 and 5, respectively

MPSO and the DE. The natural frequencies for different crack conditions generated from theoretical models are outlined in Table 3. Simulation results for four different crack conditions are presented in this paper.

Figures 7 and 8 show the convergence trend of MPSO and DE algorithms in solving the cracked beam model. It is evident from the above figure that MPSO has the faster convergence than DE in finding the optimal crack location and crack depth.

The performance of distinct methods applied for crack identification can be better compared by defining a relative percentage error that represents the difference between actual and estimated values of crack parameters. This error is defined as

$$\%\text{err}_j = \left| \frac{x_{d,j} - x_{e,j}}{x_{d,j}} \right| \times 100 \tag{15}$$

This equation is thus used in order to compare the results obtained by means of MPSO with those obtained by using DE. The results obtained in such an analysis are set forth in Table 4. It can be seen from this Table that the MPSO performs better than DE, with the mean estimation errors for crack location and crack depth being equal to 0.053 and 0.058 % for MPSO while reaching 0.251 and 0.418 % for DE, respectively.

The above study was based on the results obtained by using theoretical formulations for the cracked beam. In the following section, the results obtained by using MPSO are compared with results obtained experimentally. These latter results were obtained by considering two distinct crack locations with three different crack depths in the same test specimen. The objective function was evaluated by comparing the experimentally measured frequencies with the calculated ones. The results obtained in this way are set forth in Table 5. Although the errors obtained by comparing the theoretical results with the ones obtained experimentally are larger than those presented in Table 4, it can be concluded that MPSO performs better than DE.

This increase in relative errors may be put down to the setup of the rigid support of the cantilever beam in the experiment and to measurement errors. The mean errors for crack location and crack depth obtained from the comparison with the results obtained experimentally are equal to 8.76 and 8.78 % for MPSO and 10.396 and 10.42 % for DE, respectively. From these results, It was evident that, for the same

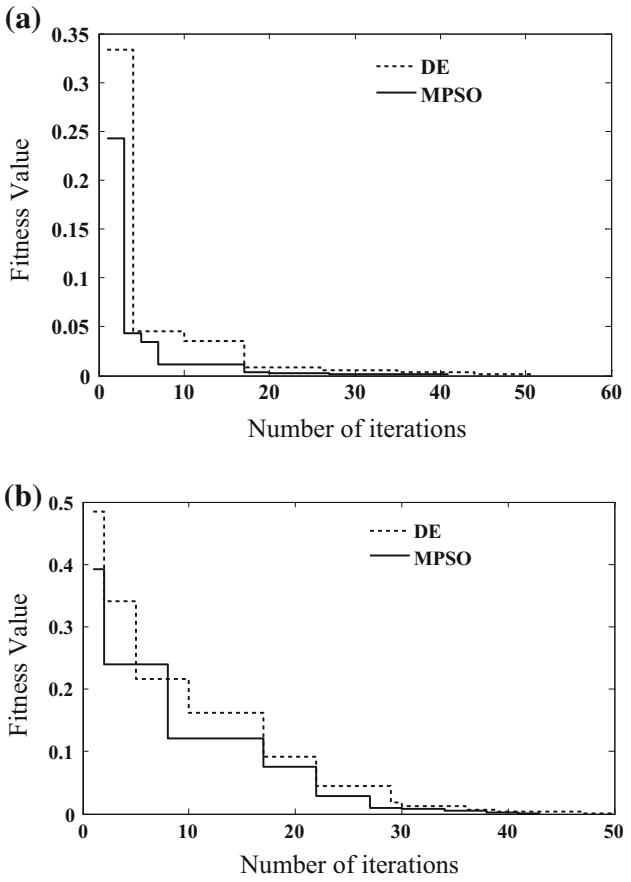

Fig. 8 **a** and **b** Convergence characteristics of MPSO and DE algorithm for crack case no. 4 and 7, respectively

crack severity, the error decreases with the increase in the distance of the crack location to beam support.

7 Conclusions

An inverse analysis of the crack identification problem in cantilever beams was examined by the application of a modified PSO (MPSO) algorithm that maintains its original structure. The squeezing strategy was incorporated in the PSO formulation in order to reduce the search domain in each iteration, thus accelerating the convergence speed for obtaining the optimal solution. The vibration signatures of the cracked beams are calculated by using the theoretical model. Reasonable changes in natural frequencies due to the presence of a crack are effectively used to identify structural damage using PSO by minimizing an objective function based on the residuals between the desired and the estimated natural frequencies. The analytical study and the experimental investigation of a cracked cantilever beam were performed to ensure the accuracy of the proposed MPSO. The dependability of the proposed algorithm was investigated by comparing the results of the MPSO with the results obtained by DE. The obtained results indicate the crack locations and crack depths were more accurately determined by the proposed algorithm than those obtained by DE. Comparisons were carried out using both the theoretical and experimental results. Based on the present study, it can be concluded

Table 4 Error estimation for crack location and depth obtained from MPSO and DE

Exact value (mm)		Predicted results (mm)							
Loc.	Dep.	MPSO				DE			
		Loc.	% Error	Dep.	% Error	Loc.	% Error	Dep.	% Error
200	1.8	200.16	0.08	1.802	0.11	199.3	0.35	1.785	0.83
200	2.4	199.88	0.06	2.398	0.08	200.56	0.28	2.412	0.50
400	1.8	400.24	0.06	1.802	0.11	398.72	0.32	1.792	0.44
400	2.4	399.80	0.05	2.4	0	400.92	0.23	2.406	0.25
600	1.8	599.76	0.04	1.801	0.05	598.86	0.19	1.794	0.33
600	2.4	600.18	0.03	2.4	0	600.84	0.14	2.404	0.16

Table 5 Error estimation results for crack location and depth in experimental study

Exact value (mm)		Predicted results (mm)							
Loc.	Dep.	MPSO				DE			
		Loc.	% Error	Depth	% Error	Loc.	% Error	Depth	% Error
50	1.2	54.87	9.74	1.316	9.67	55.71	11.42	1.338	11.50
50	1.8	54.73	9.46	1.968	9.33	55.54	11.08	2.00	11.11
50	2.4	54.51	9.02	2.617	9.04	55.34	10.68	2.656	10.66
300	1.2	274.38	8.54	1.304	8.66	269.61	10.13	1.322	10.16
300	1.8	275.49	8.17	1.948	8.22	270.72	9.76	1.975	9.72
300	2.4	276.96	7.68	2.587	7.79	272.04	9.32	2.626	9.41

that the proposed MPSO has the potential to be applied for crack detection in various structures subjected to complex loadings.

References

1. Kim, J.T.; Stubbs, N.: Crack detection in beam-type structures using frequency data. J. Sound Vib. **259**(1), 145–160 (2003)
2. Dimarogonas, A.D.; Papadopoulos, C.: Vibrations of cracked shafts in bending. J. Sound Vib. **91**, 583–593 (1983)
3. Qian, G.L.; Gu, S.N.; Jiang, J.S.: The dynamic behavior and crack detection of a beam with a crack. J. Sound Vib. **138**(2), 233–243 (1990)
4. Nahvi, H.; Jabbari, M.: Crack detection in beams using experimental modal data and finite element method. Int. J. Mech. Sci. **47**, 1477–1497 (2005)
5. Chondros, T.G.; Dimarogonas, A.D.; Yao, J.: A continuous cracked beam vibration theory. J. Sound Vib. **215**, 17–34 (1998)
6. Orhan, S.: Analysis of free and forced vibration of a cracked cantilever beam. NDT & E Int. **40**(6), 443–450 (2007)
7. Saavedra, P.N.; Cuitino, L.A.: Crack detection and vibration behavior of cracked beam. Comput. Struct. **79**, 1451–1459 (2001)
8. Zheng, D.Y.; Kessissoglou, N.J.: Free vibration analysis of a cracked beam by finite element method. J. Sound Vib. **273**(3), 457–475 (2004)
9. Rizos, P.F.; Aspragathos, N.; Dimarogonas, A.D.: Identification of crack location and magnitude in a cantilever beam from the vibration modes. J. Sound Vib. **138**(3), 381–388 (1990)
10. Gomes, H.M.; Almeida, F.J.F.: An analytical dynamic model for single cracked beams including bending, axial stiffness, rotational inertia, shear deformation and coupling effects. Appl. Math. Model. **38**, 938–948 (2014)
11. Behzad, M.; Ghadami, A.; Maghsoodi, A.; Hale, J.M.: Vibration based algorithm for crack detection in cantilever beam containing two different types of cracks. J. Sound Vib. **332**, 6312–6320 (2013)
12. Nguyen, K.V.: Mode shapes analysis of a cracked beam and its application for crack detection. J. Sound Vib. **333**, 848–872 (2014)
13. Sahoo, B.; Maity, D.: Damage assessment of structures using hybrid neuro-genetic algorithm. Appl. Soft Comput. **7**, 89–104 (2007)
14. Dash, A.K.; Parhi, D.R.: Analysis of an intelligent hybrid system for fault diagnosis in cracked structure. Arab. J. Sci. Eng. **39**, 1337–1357 (2014)
15. Aydin, K.; Kisi, O.: Damage detection in Timoshenko beam structures by multilayer perceptron and radial basis function networks. Neural Comput. Appl. **24**, 583–597 (2014)
16. Baghmisheh, V.; Taghi, M.; Peimani, M.; Sadeghi, M.H.; Ettefagh, M.M.: Crack detection in beam-like structures using genetic algorithms. J. Appl. Soft. Comput. **8**, 1150–1160 (2008)
17. Rong, H.S.; Shun, H.F.: Improving real parameter genetic algorithm with simulated annealing for engineering problem. Adv. Eng. Softw. **37**(6), 406–418 (2006)
18. Khaji, N.; Mehrjoo, M.: Crack detection in a beam with an arbitrary number of transverse cracks using genetic algorithms. J. Mech. Sci. Technol. **28**(3), 823–836 (2014)
19. Storn, R.; Price, K.: Differential evolution: a simple and efficient heuristic for global optimization over continuous spaces. J. Global Optim. **2**(4), 341–359 (1997)
20. Casciati, S.: Stiffness identification and damage localization via differential evolution algorithms. Struct. Control Health Monit. **15**, 436–449 (2008)
21. Kennedy, J.; Eberhart, R.: Particle swarm optimization. IEEE **4**, 1942–1948 (1995)
22. Samanta, B.; Nataraj, C.: Use of particle swarm optimization for machinery fault detection. Eng. Appl. Artif. Intell. **22**, 308–316 (2009)
23. Begambre, O.; Laier, J.E.: A hybrid Particle Swarm Optimization–Simplex algorithm (PSOS) for structural damage identification. Adv. Eng. Softw. **40**, 883–891 (2009)
24. Kang, F.; Li, J.; Xu, Q.: Damage detection based on improved particle swarm optimization using vibration data. Appl. Soft Comput. **12**, 2329–2335 (2012)
25. Baghmisheh, V.M.T.; Peimani, M.; Sadeghi, M.H.; Ettefagh, M.M.; Tabrizi, A.F.: A hybrid particle swarm-Nelder-Mead optimization method for crack detection in cantilever beams. J. Appl. Soft Comput. **12**, 2217–2226 (2012)
26. Mohan, S.C; Maiti, D.K; Maity, D.: Structural damage assessment using FRF employing particle swarm optimization. Appl. Math. Comput. **219**, 10387–10400 (2013)
27. Vosoughi, A.R.; Gerist, S.: New hybrid FE-PSO-CGAs sensitivity base technique for damage detection of laminated composite beams. Compos. Struct. **118**, 68–73 (2014)
28. Perera, R.; Fang, S.E.; Ruiz, A.: Application of particle swarm optimization and genetic algorithms to multiobjective damage identification inverse problems with modeling errors. Meccanica **45**, 723–734 (2010)
29. Park, J.B.; Lee, K.S.; Shin, J.R.; Lee, K.Y.: A particle swarm optimization for economic dispatch with non-smooth cost functions. IEEE Trans. Power Syst. **20**(1), 34–42 (2005)
30. Tada, H.; Paris, P.C.; Irwin, G.R.: The Stress Analysis of Cracks Hand Book. Del Research Corp., Hellertown (1973)